Plasmodium falciparum genetic crosses in a humanized mouse model

Ashley M Vaughan[1], Richard S Pinapati[2], Ian H Cheeseman[3], Nelly Camargo[1], Matthew Fishbaugher[1], Lisa A Checkley[2], Shalini Nair[3], Carolyn A Hutyra[2], François H Nosten[4], Timothy J C Anderson[3], Michael T Ferdig[2] & Stefan H I Kappe[1,5]

Genetic crosses of phenotypically distinct strains of the human malaria parasite *Plasmodium falciparum* are a powerful tool for identifying genes controlling drug resistance and other key phenotypes. Previous studies relied on the isolation of recombinant parasites from splenectomized chimpanzees, a research avenue that is no longer available. Here we demonstrate that human-liver chimeric mice support recovery of recombinant progeny for the identification of genetic determinants of parasite traits and adaptations.

Genetic crosses in the human malaria parasite *P. falciparum* have been used with outstanding success to locate the genetic determinants of important biomedical traits such as drug resistance and host specificity[1–3]. However, conducting genetic crosses with *P. falciparum* is technically difficult and expensive (**Fig. 1a**), and only three *P. falciparum* genetic crosses have been performed over a 28-year period. The biggest obstacle to routine generation of genetic crosses is the restriction of *P. falciparum* pre-erythrocytic stage development to humans and a small number of nonhuman primates including chimpanzees[4]. Moreover, the US National Institutes of Health (NIH) has recently halted the use of chimpanzees for biomedical research. Thus, a new model for genetic crossing studies would be immensely valuable for malaria genetics research. Recently, we demonstrated that a human hepatocyte-liver chimeric mouse model (the FRG huHep mouse) supports complete *P. falciparum* liver stage development, formation of exoerythrocytic merozoites and transition to asexual blood stage replication when these mice are injected with human red blood cells (huRBCs)[5]. Consequently, we predicted that the FRG huHep mouse harboring huRBCs could be used as a novel and versatile vehicle for experimental *P. falciparum* crosses.

As a proof of concept, we initially staged a cross between the documented chloroquine (CQ)-resistant strain GB4 (refs. 6,7) and a CQ-sensitive transgenic strain NF54HT-GFP–luc, which expresses a GFP-luciferase fusion[8] and is resistant to the human dihydrofolate reductase (DHFR) inhibitor WR99210 owing to transgene integration in the *pf47* locus on chromosome 13. Mature *in vitro* gametocyte cultures for both strains[9] were mixed for cross-fertilization and fed to *Anopheles stephensi* mosquitoes[10]. Sporozoites were isolated from mosquito salivary glands, and approximately 4 million sporozoites were injected intravenously into each of two FRG huHep mice. *In vivo* imaging demonstrated luciferase activity in the mouse liver indicative of parasite liver stage development[8] (**Fig. 1b**). To allow for liver stage–to–blood stage transition, we intravenously injected huRBCs into the mice twice, at 6 and 7 d after sporozoite injection—a regimen that maintains huRBC numbers in the mouse and enables initiation of *in vivo* blood stage development of transitioned parasites. Four hours after the second huRBC injection, we euthanized and exsanguinated the mice to isolate the circulating

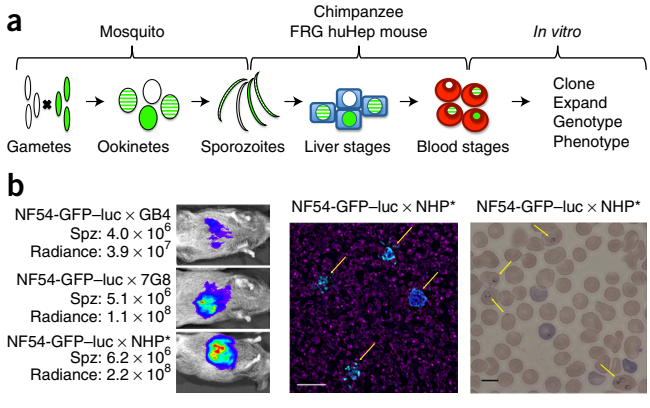

Figure 1 | The FRG huHep mouse for *P. falciparum* genetic crosses. (**a**) Schematic of experimental *P. falciparum* experimental crosses between two parasite strains (green and white) and isolation of recombinant progeny (striped). (**b**) Sporozoites (Spz) from crosses between NF54HT-GFP–luc (NF54-GFP–luc) with strains GB4, 7G8 and NHP* were injected into FRG huHep mice, and liver stage development was visualized on day 6 after inoculation by assaying luciferase activity *in vivo* (left). Liver sections from the NF54HT-GFP–luc × NHP* cross mouse were subjected to an indirect immunofluorescence assay (center), and the representative image (from analysis of ten nonserially isolated liver slices) shows the location of four liver stage parasites (yellow arrows; merozoite surface protein 1 expression shown in turquoise) in the highly humanized liver (human fumaryl acetoacetate hydrolase expression shown in magenta). DNA (blue) was stained with 4′,6-diamidino-2-phenylindole (DAPI). Scale bar, 100 µm. After liver stage–to–blood stage transition in the same cross, a representative (from 40 fields of view at 1,000×) Giemsa-stained smear (right) shows substantial blood stage parasitemia (yellow arrows point to infected red blood cells). Scale bar, 10 µm.

[1]Center for Infectious Disease Research (formerly Seattle Biomedical Research Institute), Seattle, Washington, USA. [2]Eck Institute for Global Health, Department of Biological Sciences, University of Notre Dame, Notre Dame, Indiana, USA. [3]Texas Biomedical Research Institute, San Antonio, Texas, USA. [4]Shoklo Malaria Research Unit, Mahidol-Oxford Tropical Medicine Research Unit, Mahidol University, Mae Sot, Thailand. [5]Department of Global Health, University of Washington, Seattle, Washington, USA. Correspondence should be addressed to S.H.I.K. (stefan.kappe@cidresearch.org) or M.T.F. (ferdig.1@nd.edu).

RECEIVED 30 OCTOBER 2014; ACCEPTED 21 APRIL 2015; PUBLISHED ONLINE 1 JUNE 2015; DOI:10.1038/NMETH.3432

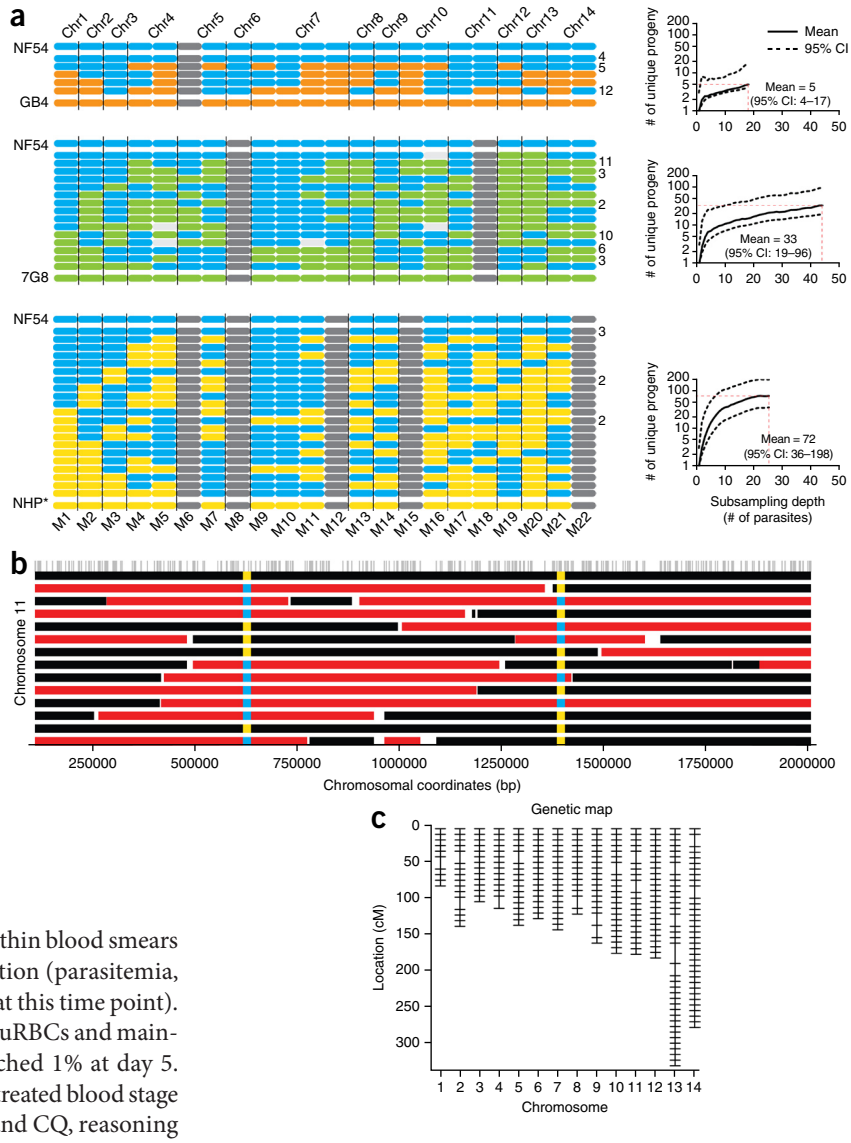

Figure 2 | Analysis of recombinant progeny from *P. falciparum* crosses. (**a**) Genotyping results for clonal progeny obtained from three experimental *P. falciparum* genetic crosses between NF54HT-GFP–luc (blue) × GB4 (orange), NF54HT-GFP–luc × 7G8 (green) and NF54HT-GFP–luc × NHP* (yellow) (crosses correspond to top, center and bottom subpanels, respectively). 22 microsatellite markers were genotyped across the 14 chromosomes (Chr). Markers in gray indicate microsatellites that were indistinguishable between the two parents. The number of cloned progeny carrying identical haplotypes is listed to the right of each haplotype; when a single haplotype was recovered, no number is listed. The rarefaction plots (right) estimate the total number of progeny present for each cross, with 95% confidence intervals (CIs) marked by dashed lines. (**b**) Detailed maps of recombination for the NF54HT-GFP–luc × NHP* cross. Patterns of inheritance for chromosome 11 are shown; see **Supplementary Figure 2** for all chromosomes. Haplotypes inherited from NHP* (black) or NF54HT-GFP–luc (red) are highlighted, with the genotypes of microsatellites superimposed onto each chromosome. The gray tick marks along the top indicate the position of the segregating single-nucleotide polymorphisms, and the scale is shown at the base. (**c**) A high-density genetic map (**Supplementary Table 3**) from the NF54HT-GFP–luc × NHP* cross was constructed using deep-sequence data.

P. falciparum–infected huRBCs. Giemsa-stained thin blood smears confirmed the liver stage–to–blood stage transition (parasitemia, i.e., the fraction of infected huRBCs, was <0.1% at this time point). We subsequently enriched infected blood with huRBCs and maintained in *in vitro* culture until parasitemia reached 1% at day 5. As an initial screen for recombinant progeny, we treated blood stage cultures with the antimalarial drugs WR99210 and CQ, reasoning that haploid parasites surviving this dual drug treatment would be recombinant, having inherited independent drug-resistant genes from each parent (mutant human *DHFR* from NF54HT-GFP–luc and the mutant *P. falciparum* CQ-resistant transporter (*pfcrt*) on chromosome 7 from GB4). Individual progeny were cloned by limiting dilution, and ten progeny (lines derived from a single infected cell) were confirmed to each carry the integration in *pf47* and the CQ-resistant mutant *pfcrt* (**Supplementary Fig. 1** and **Supplementary Table 1**). This result unambiguously demonstrates that the progeny were products of meiotic recombination.

We next performed a cross between NF54HT-GFP–luc and 7G8, a parasite line previously used in a cross to demonstrate the importance of the *pfrh5* gene in erythrocyte invasion[1]. Mature gametocyte cultures of each strain were mixed and fed to mosquitoes, and approximately 5.1 million sporozoites were injected into an FRG huHep mouse. We observed liver stage infection (**Fig. 1b**), and after liver stage–to–blood stage transition, *in vitro* blood stage parasites were cloned by limiting dilution 3 d after culture initiation. We genotyped 44 unselected progeny from this cross to evaluate Mendelian chromosomal assortment and recombination using an optimized set of 22 polymorphic microsatellites[11] spanning all 14 parasite chromosomes (**Fig. 2a** and **Supplementary Table 2**). We saw a single allele at every locus genotyped, thereby confirming the clonality of all progeny lines. The 44 unselected progeny comprised 15 independent recombinants that were represented between 1 and 11 times (**Fig. 2a**), and each unique independent recombinant varied from all other clones at a minimum of one marker. We found that six recombinant genotypes were repeated in multiple progeny (**Fig. 2a**). Of interest, we did not isolate any progeny with parental genotypes, a result indicating rare or non-existent selfing (male-female gamete pairing from the same parent). We next used rarefaction, a resampling approach widely used in ecology for estimating the numbers of species present in a community from a subsample, to estimate the total numbers of independent progeny present[12] (**Fig. 2a**). These methods estimate 33 (95% confidence interval (CI): 19–96) independent recombinants for this cross, and that just over 150 clones would need to be sampled to attain this number.

Previous crosses in chimpanzees used parasites adapted for long-term laboratory rearing, but the utility of experimental genetic crosses will be most powerfully realized using fresh parasite isolates from clinical settings to study, for instance, emerging drug resistance[13]. To explore feasibility, we produced gametocyte cultures of a recent cloned field isolate (NHP*)[14] and crossed NHP* with NF54HT-GFP–luc. After injection of approximately 6.2 million

sporozoites into a mouse, the infected liver showed a high luciferase signal (**Fig. 1b**). On liver sections taken after mouse exsanguination, indirect immunofluorescence assay using an antibody to *P. falciparum* merozoite surface protein 1 confirmed a high infection rate in the mouse (**Fig. 1b**). After the liver stage–to–blood stage transition, a Giemsa-stained smear of blood from the mouse showed a high level of huRBCs infected with *P. falciparum* ring stage parasites (**Fig. 1b**), and after only 2 d of *in vitro* blood stage culture, blood stage parasitemia reached 1%. Microsatellite analysis of the cloned progeny demonstrated the diversity of this cross: of 25 cloned progeny, we isolated 20 independent recombinants each carrying a unique allele combination (three clones carried alleles from only the NF54HT-GFP–luc parent, and only two genotypes were represented twice among the cloned progeny) (**Fig. 2a**). Rarefaction curves estimated that 72 (95% CI: 36–198) independent progeny were generated (**Fig. 2a**), and that this number of independent clones could be isolated from just over 100 cloned progeny lines.

To extend our genetic analysis further for the NF54HT-GFP–luc × NHP* cross, we sequenced the genomes of 14 independent recombinants and both parents. The parental sequences differed at 7,536 high-confidence single-nucleotide polymorphisms (SNPs), revealing 726 crossovers (**Fig. 2b**, **Supplementary Fig. 2** and **Supplementary Table 3**) in the progeny and a map length of 2,210 cM (10.4 kb/cM) (**Fig. 2c** and **Supplementary Table 3**). The proportions of SNPs inherited from each parent centered on 50% in the progeny (**Supplementary Fig. 3**), which is consistent with Mendelian expectations, and the recombination parameters are comparable to those observed in the three previous crosses using chimpanzees[11,15].

A large number of progeny carrying randomly assorting and segregating chromosomes, as well as ample recombination, are essential for high-resolution mapping of genes that confer phenotypes. From the three crosses we performed, 4, 15 and 20 independent progeny have been isolated (**Fig. 2a** and **Supplementary Table 4**). Rarefaction estimates based on the rate of discovery of new genotypes suggest that many more independent progeny can be recovered from the NF54HT-GFP–luc × NHP* cross. However, we isolated just four independent progeny from the initial NF54HT-GFP–luc × GB4 cross (**Fig. 2a**). This is likely in part due to the double-drug-selection regimen, which removes recombinants that do not carry both resistance genes. In the other two crosses, where we did not employ drug selection, the estimated numbers of progeny that could be isolated are comparable (NF54HT-GFP–luc × 7G8) (**Fig. 2a**) or exceed (NF54HT-GFP–luc × NHP*) (**Fig. 2a**) those isolated from previous chimpanzee crosses[11,15]. We speculate that the success in deriving large number of recombinants from the NF54HT-GFP–luc × NHP* cross (**Fig. 2a** and **Supplementary Table 4**) in part resulted from the use of a highly transmissible parasite that we recently isolated from a patient. Whole-genome sequencing of 14 progeny from the NF54HT-GFP–luc × NHP* cross revealed recombination patterns characteristic of previous crosses conducted using chimpanzees, thus demonstrating the power of the FRG huHep mouse model to yield *P. falciparum* progeny for linkage mapping (**Fig. 2b** and **Supplementary Fig. 2**). Further optimization of the procedures described will improve the efficiency with which recombinant progeny are recovered.

The spread of artemisinin (ART) resistance in southeast Asia[13] is an emergent crisis in malaria control. Population genetics and a 5-year laboratory selection of ART-resistant parasites led to the discovery of a marker for ART resistance, the Kelch locus[14,16,17]. The methodology presented here could have significantly accelerated the identification of this marker. Well-defined genetic crosses between ART-resistant and susceptible strains now promise to improve our understanding of the genetic and functional underpinnings of ART resistance. Furthermore, staging *P. falciparum* genetic crosses using the FRG huHep mouse model provides a powerful framework for integrated analysis of multiple layers of genomic-scale data ('systems genetics') to better understand biomedically important parasite traits.

METHODS

Methods and any associated references are available in the online version of the paper.

Accession codes. NCBI Sequence Read Archive: whole-genome sequences have been deposited under accession number PRJNA278779.

Note: Any Supplementary Information and Source Data files are available in the online version of the paper.

ACKNOWLEDGMENTS

We thank the Center for Infectious Disease Research (formerly Seattle BioMed) insectary and vivarium for mosquito and rodent care, respectively, as well as R. Garcia and M. McDew-White at the Texas Biomedical Research Institute for technical assistance. We thank S. Mikolajczak, E. Wilson and J. Bial for ongoing FRG huHep mouse discussions and M. Macarulay and K. Ushimaru for help with parasite cloning. Thanks also to A. Kaushansky for help with graphics. NIH grants R21 AI 115194–01 to A.M.V. and M.T.F., R37 AI 048071 to T.J.C.A. and Chemistry-Biochemistry-Biology Interface Training Fellowship T32 GM075762 to R.S.P. supported this work, as did Seattle BioMed internal funds to S.H.I.K. The AT&T Genomics Computing Center at Texas Biomedical Research Institute is supported by the AT&T Foundation and the US National Center for Research Resources (NCRR) grant number S10 RR029392, and laboratory work was conducted in facilities constructed with support from Research Facilities Improvement Program grant C06 RR013556 and RR017515 from NCRR.

AUTHOR CONTRIBUTIONS

A.M.V., S.H.I.K. and M.T.F. conceived, initiated and supervised the project. A.M.V., S.H.I.K., T.J.C.A., R.S.P. and M.T.F. designed experiments and wrote the manuscript. A.M.V., N.C., M.F., L.A.C., R.S.P., I.H.C., S.N. and C.A.H. carried out the experiments. F.H.N. and T.J.C.A. supplied parasites. A.M.V., S.H.I.K., I.H.C., T.J.C.A., R.S.P. and M.T.F. analyzed results.

COMPETING FINANCIAL INTERESTS

The authors declare no competing financial interests.

1. Hayton, K. *et al. Cell Host Microbe* **4**, 40–51 (2008).
2. Ranford-Cartwright, L.C., Hayton, K.L. & Ferdig, M.T. in *Malaria Parasites: Comparative Genomics, Evolution and Molecular Biology* (eds. Carlton, J.M., Perkins, S.L. & Deitsch, K.W.) Ch. 6, 127–144 (Caister Academic Press, 2013).
3. Walliker, D. *et al. Science* **236**, 1661–1666 (1987).
4. Rodhain, J. & Jadin, J. *Ann. Soc. Belges Med. Trop. Parasitol. Mycol.* **44**, 531–535 (1964).
5. Vaughan, A.M. *et al. J. Clin. Invest.* **122**, 3618–3628 (2012).
6. Sá, J.M. *et al. Proc. Natl. Acad. Sci. USA* **106**, 18883–18889 (2009).
7. Sullivan, J.S. *et al. Am. J. Trop. Med. Hyg.* **69**, 593–600 (2003).
8. Vaughan, A.M. *et al. Mol. Biochem. Parasitol.* **186**, 143–147 (2012).
9. Trager, W. & Jensen, J.B. *Science* **193**, 673–675 (1976).
10. Kaushal, D.C., Carter, R., Miller, L.H. & Krishna, G. *Nature* **286**, 490–492 (1980).
11. Su, X. *et al. Science* **286**, 1351–1353 (1999).
12. Colwell, R.K. *et al. J. Plant Ecol.* **5**, 3–21 (2012).
13. Dondorp, A.M. *et al. N. Engl. J. Med.* **361**, 455–467 (2009).
14. Cheeseman, I.H. *et al. Science* **336**, 79–82 (2012).
15. Jiang, H. *et al. Genome Biol.* **12**, R33 (2011).
16. Ariey, F. *et al. Nature* **505**, 50–55 (2014).
17. Takala-Harrison, S. *et al. Proc. Natl. Acad. Sci. USA* **110**, 240–245 (2013).

ONLINE METHODS

Study approval. The study was performed in strict accordance with the recommendations in the Guide for the Care and Use of Laboratory Animals of the National Institutes of Health (NIH), USA. To this end, the Center for Infectious Disease Research has an Assurance from the Public Health Service (PHS) through the Office of Laboratory Animal Welfare (OLAW) for work approved by its Institutional Animal Care and Use Committee (IACUC). The PHS Assurance number is A3640-01. All of the work carried out in this study was specifically reviewed and approved by the Center for Infectious Disease Research IACUC.

FRG NOD huHep mice. Male and female FRG NOD huHep mice[18] with human chimeric livers were purchased from Yecuris Corporation. The mice are immunocompromised and should ideally be maintained in a barrier facility. In our hands, the mice were healthy throughout the course of experimentation. For each of the experimental genetic crosses performed, one or two FRG huHep mice were used for liver stage development and subsequent liver stage–to–blood stage transition. The mice were not formally randomized, nor were researchers blinded, before injection. No sample-size estimation was performed as there are no statistics presented where we try and detect an effect size between groups. The mice injected intravenously with *P. falciparum* sporozoites from the NF54HT-GFP–luc × GB4 cross and the NF54HT-GFP–luc × 7G8 cross were male and 6 months of age, and the mouse that received sporozoites from the NF54HT-GFP–luc × NHP* cross was female and 7 months of age. The mice had human albumin levels between 4.3 and 7.3 mg/mL. Mice used in the study were supplemented with NTBC at 8 mg/L in their drinking water on arrival and maintained on this dose until euthanasia.

***P. falciparum* sporozoite production and liver stage infection.** The *A. stephensi* mosquitoes used in this study were maintained at 27 °C and 75% humidity on a 12-h light/dark cycle. We followed MR4 protocols for larval stage and adult stage rearing; to this end, larvae were fed with finely ground Tetramin fish food, and adults were fed with cotton balls soaked in a solution of 8% dextrose and 0.05% para-aminobenzoic acid in water.

P. falciparum blood stage cultures were maintained *in vitro* in standard cell culture RPMI-1640 with 25 mM HEPES and 2 mM L-glutamine supplemented with 50 µM hypoxanthine and 10% A^+ human serum. An atmosphere of 5% CO_2, 5% O_2 and 90% N_2 was used for growth, and infected *P. falciparum* red blood cells were subcultured into O^+ erythrocytes.

To initiate sexual stage development, we set up early passages (no more than ten passages) of asexual cultures at a parasitemia between 0.8% and 1% (mixed stages) and 5% hematocrit and maintained them with daily medium changes for up to 17 d. Mature gametocytes were fed to adult female mosquitoes 3- to 7-d post-emergence. To do this, gametocyte cultures were pelleted for 3 min at 800*g* and diluted to a 40% hematocrit using fresh A^+ human serum and O^+ erythrocytes at 37 °C. Mosquitoes were allowed to feed for 20 min, and the blood was maintained at 37 °C throughout.

Mosquitoes were maintained for up to 19 d, and the prevalence of infection was analyzed between days 7 and 10 by examining dissected midguts under light microscopy for the presence of oocysts. Salivary gland dissections were performed at days 14–19, and sporozoite numbers were enumerated using a hemocytometer. In order to minimize the deleterious effects of salivary gland extract injection into the mice, we used average sporozoite numbers per mosquito >30,000. Additionally, salivary gland dissection was performed to minimize the isolation of extraneous mosquito material.

Mice were injected intravenously into the tail vein with between approximately 4.0 million and 6.2 million *P. falciparum* salivary gland sporozoites in 200 µL of RPMI medium without supplements. Six days after sporozoite injection, liver stage luciferase activity was visualized (**Fig. 1b**) through imaging of whole bodies using the IVIS Lumina II animal imager (Caliper Life Sciences). Mice were injected with 100 µL of RediJect D-luciferin (PerkinElmer) intraperitoneally before being anesthetized using an isoflurane anesthesia system (XGI-8, Caliper Life Sciences). Animals were kept anesthetized during the measurements, which were performed within 5–10 min after the injection of D-luciferin. Bioluminescence imaging was acquired with a 10-cm FOV, medium binning factor and an exposure time of 5 min. Quantitative analysis of bioluminescence was performed by measuring the luminescence signal intensity using the ROI settings of the Living Image 3.0 software.

Liver stage–to–blood stage transition and *in vitro* culture of blood stages derived from FRG NOD huHep mouse infections. We have determined that the majority of liver stage parasites fully mature and release exoerythrocytic merozoites between 6 and 6.5 d after sporozoite infection. To maximize the number of transitioned ring stage parasites for downstream analysis, we injected mice with huRBCs twice before exsanguination: once at 6 d after sporozoite injection and a second time at 7 d after sporozoite injection. A second injection of huRBCs is performed to catch late-transitioning liver stage parasites. Some huRBCs injected into the mice are cleared by the spleen, but the majority survive *in vivo*, and thus liver stage parasites that mature and release exoerythrocytic merozoites after huRBC injection have the potential to invade huRBCs and begin to develop *in vivo* in the mouse. To this end, 6 d after sporozoite injection, we injected mice intravenously with 400 µL of packed O^+ huRBCs. The intravenous injection was repeated on day 7. Four hours after the second huRBC injection, mice were sacrificed and blood was removed by cardiac puncture in order to recover *P. falciparum*–infected huRBCs. The blood was added to 10 mL complete medium (RPMI-1640 with 25 mM HEPES, 2 mM L-glutamine, 50 µM hypoxanthine and 10% A^+ human serum) and pelleted by centrifugation at 200*g*. The supernatant along with the buffy coat (containing white blood cells) were then removed, and the red blood cells were washed three times with 10 mL complete medium, with pelleting and centrifugation as detailed above. After the third wash, an equal volume of packed O^+ huRBCs (approximately 400 µL) was added, and the total RBC pellet was resuspended in complete medium to 2% hematocrit. Cultures were split equally into six wells of a standard six-well plate and maintained in an atmosphere of 5% CO_2, 5% O_2 and 90% N_2. Cultures were fed daily, and 50 µL of freshly packed huRBCs were added every 5 d to each well. Once parasitemia reached 1%, serial dilutions of parasites were carried out to maintain healthy cultures. Additionally, cloning of parasites by limiting dilution was carried out in standard 96-well plates.

doi:10.1038/nmeth.3432

Immunofluorescence assay (IFA). After mouse exsanguination at a time point when the majority of liver stage parasites have matured and released exoerythrocytic merozoites, the liver was perfused with phosphate-buffered saline (PBS) through the hepatic portal vein, removed, separated into lobes and fixed in 4% electron microscopy–grade formaldehyde in PBS, which was replaced by Tris-buffered saline (TBS) + 0.05% (w/v) sodium azide after 24 h. The fixed lobes were subsequently sliced into 50-µm sections for IFA, as detailed previously[19]. *P. falciparum* liver stages were detected with a mouse monoclonal merozoite surface protein 1 (MSP1) antibody (MRA-476) (1:1,000 dilution). MRA-476 was obtained through the MR4 as part of the BEI Resources Repository, NIAID, NIH: *Mus musculus* (B cell); *Mus musculus* (myeloma) S1-3D6, MRA-476, deposited by C.A. Long. Human hepatocytes were detected with a rabbit polyclonal antibody (1:1,000 dilution) to human fumaryl acetoacetate hydrolase (FAH) obtained from the Yecuris Corporation (catalog number 20-0034). Fluorescent Alexa Fluor 594 goat anti-mouse IgG and Alexa Fluor 488 goat anti-mouse IgG (Life Technologies) secondary antibodies were diluted 1:500. MSP1 expression can be detected in mature liver stage parasites and also at the localization of liver stage parasites that have previously released exoerythrocytic merozoites. This is due to the fact that residual MSP1 is seen at the site of merozoite release. Performing this IFA allows for an assessment of the success of the sporozoite infection and downstream liver stage development in the mouse. The DeltaVision Elite System 1 package was used for image capture following IFA. This encompasses an Olympus IX71 microscope to which a Photometrics Cool SNAP HQ^2 camera is attached. A 7 Color Combined InsightSSI provided with the system provides ultrafast solid-state illumination without filter changes. The image in **Figure 1b** (center panel) was captured using an Olympus UPlanFL N 10× objective at room temperature. Use of the softWoRx 6.1.3 Software Suite allowed for image deconvolution, and a single *xyz* image was pseudocolored turquoise (MSP1), magenta (FAH) and blue (DNA) for the purposes of this publication.

PCR and RFLP analysis of clones from the NF54HT-GFP–luc × GB4 cross. Transitioned blood stage parasites were cultured with the addition of 50 nM CQ for 5 d and subsequently for a further 7 d with 5 nM WR99210. The CQ- and WR99210-resistant parasites were then cloned by limiting dilution and seeded at 0.5 parasites per well in 96-well plates. A total of ten clones were initially recovered.

Genomic DNA from the NF54HT-GFP–luc and GB4 parents and recombinant progeny was isolated and subjected to PCR using primers specific to the 5′ and 3′ *pf47* integration site for the GFP–luc expression cassette. Additionally, PCR primers that flanked the mutated allele within *pfcrt* were used for RFLP analysis following digestion with ApoI. Primers used for the study are listed in **Supplementary Table 1**.

Microsatellite analysis of recombinant progeny. Microsatellite (MS) markers were developed on the basis of several criteria. All MS markers were first described in the high-resolution linkage map for *P. falciparum*[11]. Initially, 35 MS markers were selected for genome-wide representation and because the literature[6,20] indicates that they can detect sufficient polymorphism. These were evaluated to arrive at an optimized and informative set of 22 MS markers (**Supplementary Table 2**). The four parasites serving as parents (NF54HT-GFP–luc, GB4, 7G8 and NHP*) and the progeny resulting from the genetic crosses were grown under standard culture conditions[21]. Genomic DNA extracted from all the parasites using the phenol-chloroform method was PCR amplified using the Phusion Flash High-Fidelity PCR Master Mix (Thermo Scientific) and fluorescently labeled primers (Sigma-Aldrich) specific to the 22 MS markers distributed across the 14 chromosomes of *P. falciparum*. The PCR reaction mixtures were subjected to an initial denaturation at 98 °C for 10 s followed by 30 cycles of denaturation at 98 °C for 1 s, annealing at 48–58 °C for 5 s, extension at 65 °C for 15 s, and a final extension at 65 °C for 1 min. Primers for the MS markers used for genotyping are listed in **Supplementary Table 2**. The amplified products were analyzed on a CEQ 8000 Genetic Analysis System (Beckman Coulter).

Abundance of independent recombinants. We applied rarefaction, originally developed by ecologists to estimate the numbers of species present in a community, to estimate the number of recombinants generated by each cross using EstimateS v9.0.0 (http://viceroy.eeb.uconn.edu/estimates/). We used individual-based curves and sampling without replacement to estimate the number of recombinants present. The results present were from Chao's formula 1, though identical results were obtained using the ACE estimator. In addition, we estimated the numbers of clones that would need to be sampled to obtain the estimated numbers of recombinants present.

Illumina sequencing and analysis of recombination parameters. Two micrograms of DNA were sheared using a Covaris S-series sonicator (Covaris; duty cycle, 20%; time, 180 s; intensity, 5; cycle burst, 200; power, 37 W; temperature, 7 °C; mode freq, sweeping) from the two parents (NF54HT-GFP–luc × NHP*) and 14 recombinant progeny from the cross. After end repair and A-tailing, multiplex-indexed adaptors were ligated to sheared DNA using NEBnext library preparation kits for Illumina (New England BioLabs). Agencourt AMPure XP beads (Beckman Coulter) were used for sample purification between steps, and the Kapa HiFi DNA polymerase (Kapa Biosystems) was used for amplifications[22,23]. Templates were quantified using the Kapa SYBR Fast ABI Prism qPCR kit (Kapa Biosystems). Thirteen samples were multiplexed per lane and sequenced on an Illumina HiSeq 2500. CASAVA 3.0 was used to demultiplex raw sequence data and fastq .files generated before further analysis.

We mapped 101-bp paired-end reads from .fastq files against the *P. falciparum* genome reference strain 3D7 v9.2 (http://plasmodb.org/common/downloads/release-9.2/Pfalciparum3D7/fasta/data/) using BWA v0.6.1 (ref. 24). Reads that map off chromosome ends and PCR duplicates were removed from BAM files using Picard v1.56 (http://broadinstitute.github.io/picard/) Realignment around indels and base-quality scores were recalibrated using the Genome Analysis Toolkit v2.3-9 (ref. 25). Final SNP calling was performed using the UnifiedGenotyper, which was followed by variant quality-score recalibration. We excluded variants by evaluating standard quality metrics (QUAL < 100.0, FS < 50, BaseQRankSum $-2 > X > 2$, MQRankSum $-2 > X > 2$, QD < 10).

A genetic map was constructed using the est.map function in R/qtl[26] in R v3.1.0 using the Haldane map function. As the parental lines were sequenced directly, each SNP in the progeny was designated by its parent of origin. We calculated pairwise allele sharing between progeny using the comparegeno function, and we assessed whether the observed data conformed to a normal distribution using the Shapiro-Wilk test for normality, implemented in the shapiro test function in R.

18. Azuma, H. *et al. Nat. Biotechnol.* **25**, 903–910 (2007).
19. Vaughan, A.M. *et al. Cell. Microbiol.* **11**, 506–520 (2009).
20. Mita, T. & Jombart, T. *Parasitol. Int.* **64**, 238–243 (2015).
21. Reilly Ayala, H.B., Wacker, M.A., Siwo, G. & Ferdig, M.T. *BMC Genomics* **11**, 577 (2010).
22. Oyola, S.O. *et al. BMC Genomics* **13**, 1 (2012).
23. Quail, M.A. *et al. Nat. Methods* **9**, 10–11 (2012).
24. Li, H. & Durbin, R. *Bioinformatics* **25**, 1754–1760 (2009).
25. DePristo, M.A. *et al. Nat. Genet.* **43**, 491–498 (2011).
26. Broman, K.W., Wu, H., Sen, S. & Churchill, G.A. *Bioinformatics* **19**, 889–890 (2003).

doi:10.1038/nmeth.3432